APPENDIX E

Development of a Prediction Scheme for High Aspect-Ratio Jet Noise

APPENDIX E

Development of a Prediction Scheme for High Aspect-Ratio Jet Noise

Scott E. Munro*
and
K. K. Ahuja
Georgia Institute of Technology
GTRI/ATASL
Atlanta, GA, 30332-0844

Abstract

Circulation control wings are a type of pneumatic high-lift device that have been extensively researched as to their aerodynamic benefits. However, there has been little research into the possible airframe noise reduction benefits of a circulation control wing. The key element of noise is the jet noise associated with the jet sheet emitted from the blowing slot. This jet sheet is essentially a high aspect-ratio rectangular jet. A recent study on high aspect-ratio jet noise was performed on a nozzle with aspect-ratios ranging from 100 to 3,000. In addition to the acoustic data, fluid dynamic measurements were made as well. This paper uses the results of these two studies and attempts to develop a prediction scheme for high aspect-ratio jet noise.

Nomenclature

A -- Area (typically of nozzle)
AR -- Aspect ratio
a -- Speed of sound
a_o -- Ambient speed of sound
D -- Diameter of round jet exit
d_{eq} -- Equivalent diameter, $2(A/\pi)^{1/2}$
F -- Tam's large scale turbulence generic acoustic spectrum, function of (f/f_p)
f -- Frequency
f_p -- Peak frequency
G -- Tam's fine scale turbulence generic acoustic spectrum, function of (f/f_p)
HARN -- High aspect-ratio nozzle
h -- Slot height or rectangular nozzle height (small dimension)
I -- Sound intensity
L -- Characteristic length
L_{eq} -- Characteristic length for the HARN, $L_{eq} = h^{3/4}w^{1/4}$
M_c -- Convection Mach number
M_o -- Jet centerline Mach number
P -- Sound power
P_{ref} -- Reference acoustic pressure, 20 μPa
p -- pressure
q -- $\frac{1}{2}\rho V^2$ (dynamic pressure)
R -- Radial distance from jet exit to measurement location
SPL -- Sound Pressure Level
T -- Temperature
T_{ij} -- Stress tensor, $\rho u_i u_j + p_{ij} - a_o^2 r\delta_{ij}$
w -- width of rectangular nozzle (large dimension)
V -- Velocity
V_c -- Turbulent eddy convection velocity
V_j -- Jet exit velocity (fully expanded)
V_t -- Local jet centerline velocity
x -- Streamwise dimension, typically x = 0 is nozzle exit
y -- Dimension perpendicular to major axis of nozzle, y = 0 is center of nozzle
z -- Dimension along span of nozzle (parallel to major axis), z = 0 is center of nozzle
Θ -- Angle of measurement with respect to the flow axis
ρ -- density

Introduction

This paper uses the results of a recently-completed aeroacoustics study of a High Aspect-Ratio Nozzle (HARN) performed at Georgia Tech Research Institute (GTRI) to develop an empirical noise prediction scheme of jet noise from such nozzles. Results of this studiy can be found in references 1 –3. General trends in the HARN acoustic data were examined in reference [1]. In this process, the available round jet experimental trends and theory were used as a starting point. It was found that the HARN data followed the V_j^8 law similar to round jets and data from low-aspect-ratio rectangular nozzles.[1]

While round jet noise follows D^2 and researchers have had some success scaling low aspect-ratio rectangular jet noise based on an equivalent diameter, $D_{eq} = (4hw/\pi)^{1/2}$, the HARN data did not collapse using D_{eq} as the characteristic length.[1] Lighthill's estimation of jet noise developed for round jets results in the intensity of the noise being proportional to D^2. The use of diameter for round jets comes from the fact that the turbulent eddy volume

* Now works for the Naval Air Warfare Center, Weapons Division, China Lake, CA 93555-6100.

and frequency of the turbulence are related to the jet diameter.

In the case of the HARN, it was found that the height and width tend to affect the amplitude and frequency of the jet noise differently. The intensity of the sound was found to be proportional to $h^{3/2}$ for the lower aspect-ratio geometries and proportional to h^2 for the higher aspect ratios. The width was found to have little effect on the SPL for low aspect ratios, however the intensity was found to proportional to the width for the high aspect ratios.

Initially, rather than develop a complex relationship for the exponents for h and w dependent on aspect-ratio, a "best fit" relationship using constant exponents was sought. The best length scale that provided the noise intensity for the HARN proportional to the square of the length scale was found to be $L_{eq} \sim h^{3/4}w^{1/4}$. This characteristic length-scale was used to non-dimensionalize the frequency of the acoustic spectra as well as to collapse the amplitude. For constant jet velocity, this scheme collapses the data reasonably well at most polar angles.[1]

The above definition of the length-scale, namely $L_{eq} \sim h^{3/4}w^{1/4}$ and the result that the V_j^8 law was valid for $\Theta = 90^o$ were used to collapse the HARN data at that polar angle. Figure 1 contains a sample of the unscaled and scaled data to show the reasonable effectiveness of the scaling parameters developed in reference [1]. While the data collapse is not perfect, this simple scheme does scale the data reasonably well over a wide range of nozzle conditions.

One area where this scheme, as well as prediction schemes for round jets, fails is in the prediction of the amplitude and frequency content of the noise radiated at the low polar angles. Lighthill's analogy does include a Doppler term to account for moving turbulent eddies, however it has been found that there is a significant amount of turbulence scattering of high frequency noise for polar angles below 50°.[4-5] This was found to have a large effect on the HARN data. However, as a result, the prediction schemes often used do not properly account for this effect. Tam and his colleagues contend that there is a different reason why low polar angles do not have similar noise characteristics to higher angles. They believe that there are two distinct types of noise radiating from two distinct sources within the flow.[6-13]

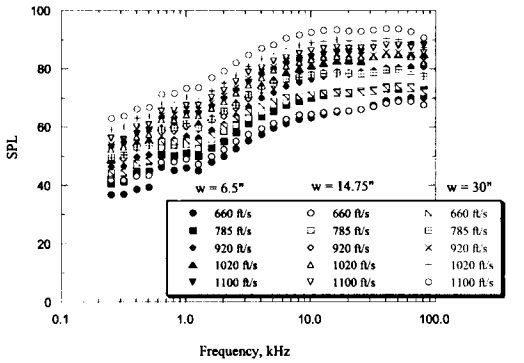

(a)

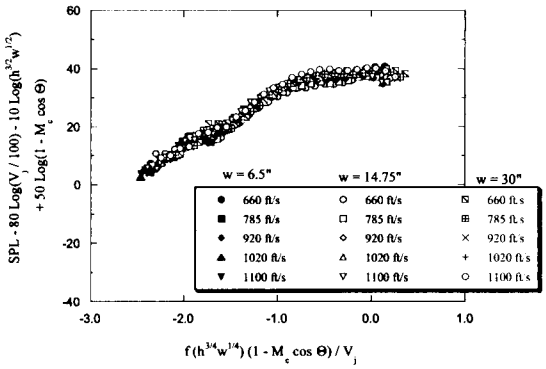

(b)

Figure 1: Typical HARN acoustic data, (a) Raw data, (b) Collapsed data.

In addition to the problems associated noise at various polar angles, the flow study (reference [2]) on the HARN revealed some interesting results that may yield some insight into the discrepancies between data and the predictions. These include the sudden bursting of the jet some distance downstream of the nozzle exit as found in our PIV and hot-wire results and the fact that convection velocity is dependent on the centerline velocity rather than the jet exit velocity. The convection velocity was also found to be a function of the frequency of the turbulence. Also, global length-scale calculations supported the L_{eq} definition from the acoustic study.[2]

These results and the general jet flow characteristics are used below to enhance the prediction scheme for high aspect-ratio rectangular jet noise. Attempts are also made to relate HARN data to round data using a common prediction scheme that is relevant to all nozzles. And finally, the HARN data is compared with the predictions using schemes developed by Tam et al.[6-13]

APPENDIX E

Review of Jet Noise Theories, Experiments, and Prediction Schemes

Jet Noise from Round Nozzles

As soon as jet and rocket engines began making their way into the aircraft designs, the noise from these new types of engines became an issue. In some cases it was more for controlling damage, such as in the case of a rocket launch, where the launch area is subjected to a large amount of noise from the rocket motors during the launch. The other major issue came with increased jet travel and jet aircraft activity around airports. The new jet aircraft were much louder and more annoying to the surrounding population.

Thus, research into jet noise soon began to emerge. Much of the early theoretical gains in jet noise prediction came from Lighthill's work on round jets. Various versions of this work are found in references.[14-17] Lighthill derived equations for a turbulent flow including Reynolds stresses and the associated turbulent terms. He also showed that the dominant stress term was $\rho v_i v_j$ at low Mach numbers. Since turbulent fluctuations correlate well for points within a volume on the scale of the typical eddy size, Lighthill proposed that acoustic sources associated with the turbulent fluctuations at these points were coherent. Thus, the distribution of quadrupole sources in the volume radiated sound similar to a single quadrupole equal in strength to the combined distribution. Essentially the noise associated with a particular eddy is represented by a quadrupole source. Lighthill went on to assume that the jet flow was made up of a number of eddies, and thus a similar number of these point quadrupoles representing eddies. From this physical model, several relationships were derived, including 'Lighthill's eighth power law' relationships for the sound intensity and the sound power

$$: I \sim \frac{\rho_m^2 V_j^8 D^2}{\rho_o a_o^5 R^2} \text{ and } P \sim \frac{\rho_m^2 V_j^8 D^2}{\rho_o a_o^5}. \quad (1)$$

The derivation shown above has mostly been applied to round jets of diameter D.[14-17] Secondly, there are important relations that are shown, specifically that the sound intensity is proportional to the eighth power of velocity and inversely proportional to the square of the radius between the source and observer. The final note on these equations is that they also assume that the eddies (or quadrupoles) convected at a very low Mach number. When the eddies are convected at a higher Mach number (M_c) the analysis must take this into account by shifting to the reference frame of the convecting eddy. When backed out to the observer, the equations change to

$$I \sim \frac{\rho_m^2 V_j^8 D^2}{\rho_o a_o^5 R^2} (1 - M_c \cos(\Theta))^{-5} \text{ and}$$

$$P \sim \frac{\rho_m^2 V_j^8 D^2}{\rho_o a_o^5} \frac{(1 + M_c^2)}{(1 - M_c^2)^4}. \quad (2)$$

In the intensity equation, Θ is the angle of the observer with respect to the downstream jet axis. These equations predict the amplitude of jet noise, but say nothing of frequency.

However, one can again go back to the eddy which is essentially the driving force behind the noise. Near the exit of the nozzle where the mixing region is small, the turbulence is dominated by small eddies, thus higher frequency noise is associated with the small length scale. As the shear layer grows, the larger eddies further downstream are believed to be responsible for lower frequency jet noise.[4] But notice that these characteristics are dependent on the geometry and mixing characteristics of the jet. Thus, the frequencies must also scale in order to be able to predict the entire spectrum of jet noise. The frequency scaling is taken into account by non-dimensionalizing the frequency into a Strouhul number and accounting for the moving sources. This relation is

$$\frac{fD}{V}(1 - M_c \cos\Theta) \quad (3)$$

Most of Lighthill's theory has been experimentally verified for round jets. One key study in this area was performed by Ahuja, and Ahuja and Bushell.[4,5] They made careful measurements of jet noise for 3 different diameter round jets. An effort was made to eliminate all other possible sources of noise, such as valve and flow noise from upstream in the nozzle system. Ahuja verified the data by scaling all his data to the same condition, which would collapse all the data if Lighthill's theory was correct. This was a fairly straightforward process when working with sound pressure levels. Since the sound pressure level (SPL) is defined as

$$SPL = 10 \log\left(\frac{I}{I_{ref}}\right) \quad (4)$$

where $I_{ref} = 10^{-12}$ W/m^2. Thus, if the intensity is normalized by some "standard" intensity and a "standard" SPL is solved for, the result is[4]

$$"standard" SPL = SPL - 10 \log\left(\frac{V}{V_s}\right)^8 - 10 \log\left(\frac{D}{D_s}\right)^2 + 10 \log\left(\frac{R}{R_s}\right)^2 - 10 \log(1 - M_c \cos\Theta)^{-5} \quad (5)$$

where the variables with an 's' subscript signify conditions of the "standard" case, i.e. V_s = 100 ft/s, D_s = 1", R_s = 10 ft. Θ_s is typically 90°, so the reference value in the final term becomes 1 and is therefore not shown. Thus, any SPL measurement from a jet could be transformed, or scaled to the SPL for this standard case. If Lighthill's theory holds, then jet noise from experiments could all be collapsed into one curve by plotting the "standard" SPL for all data versus the normalized frequency. This is very powerful information since the reverse could be done as well. The 'Standard SPL' data could be scaled using a geometry, distance, or velocity to predict what the noise would be in that case. Ahuja's experimental data for unheated jets agreed with many of Lighthill's predictions but did not match in all cases. Even so, Lighthill's theory has until recently remained the basis for developing jet noise prediction schemes and extrapolating noise from one system to another by using the velocity, diameter, and radius factors derived in the above equations. Recently Lighthill's theory based on acoustic analogy has come under much scrutiny and some other jet noise theories have come to the forefront. One of those theories has been put forth by Tam and several other researchers.[6-8,12] Tam suggests that there are two different noise mechanisms, one that is associated with the large scale turbulence and other with the fine scale turbulence.[6,7,12] Tam and Auriault also claim that these two mechanisms dominate the acoustic jet noise spectra in different regions of the polar arc. Specifically, the large scale turbulence noise dominates the spectrum at small polar angles, while the fine-scale turbulence dominates the spectrum at higher polar angles.[6,7,12] References [6-8,12] describe two generic noise spectra, one for each type of noise. In addition to the spectra, empirical amplitude formulas have been developed that account for differences in jet velocity, temperature and diameter. These generic spectra have been applied to a wide variety of jet noise data with reasonable success.[6-8,12]

It is apparent that even in the case of the well studied round jet, there is still discussion of the appropriate theory and scaling. This is also true of jet noise rom non-round nozzles and more complex suppressor nozzles.. This is particularly true in the case of rectangular jets where there has not been nearly the focus given to round jets. The following section discusses in some detail the differences found between the round jet case and rectangular jet case.

Jet Noise From Rectangular Nozzles

Although round nozzles dominated most of the applications where jet noise was of interest, there have always been some applications where a rectangular nozzle is more appropriate. Thus, there has also been some work on the topic of rectangular jet noise.

Almost all work on jet noise was conducted on round jets until there were applications where a non-axisymmetric shape had advantages over an axisymmetric nozzle. The first rectangular nozzle work strictly for noise reduction appears to have been performed performed by Tyler, et al.[18] Other applications were more thrust related. Rectangular nozzles produced better performance at higher Mach numbers in military aircraft tests.[19,20] However, the rectangular nozzles in these applications typically had aspect-ratios from 2 – 7.[21] These early studies were typically also limited to higher subsonic or supersonic Mach numbers.[22] Other examples of very early studies are Maglieri and Hubbard's work on jets of different aspect-ratios,[23] and Cole's work on high aspect-ratio slot-noise.[24] Maestrello and McDaid investigated slot jets with aspect-ratios from 5 to 20.[25] Gruschka and Schrecker[26] and Schrecker and Maus[27] investigated the noise emitted from high aspect-ratio slot jets. One of the major motivations behind this work was the fact that jet velocity of rectangular jets decayed at a higher rate compared with round jets, thus resulting in a lower sound energy.[28] However, in all these works high aspect-ratio referred to aspect-ratios typically at least an order of magnitude lower (sometimes two orders of magnitude) than the HARN jet investigated in the present work.[21,26,27]

The research on rectangular nozzles has produced some differing results. The acoustic power dependence of V_j^8 for round circular jets has been found by some researchers[48] while V_j^7 has been reported by others[22,27,29] The work documented in references [25,26] found that the jet velocity dependence was actually a function of the aspect-ratio of the jet. The range of aspect-ratios tested were from 30 to 120, and the velocity scaling function ranged from V_j^6 to V_j^7.

Ffwocs-Williams suggested in reference [29] that the exit geometry can affect the noise by an additional component he termed "lip noise." The lip noise radiates as a fluctuating force dipole source. Typically, the dipole source radiates noise proportional to V_j^6. Reference [21] speculated that this noise combined with the turbulent mixing noise produced the V_j^7 relationship found in their investigation.

Kouts and Yu[22] also noted that the peak frequency of the spectra only had a week dependence on jet velocity. They also found that the rectangular jet seemed to have more high frequency content than circular jets.[22] Also, in contrast to round jets, researchers have found that the peak frequency has a weak dependence on the nozzle height.[22,26,27] This was unexpected since round jets have a strong dependence

on jet diameter and the nozzle height is the appropriate scale for the initial mixing region in rectangular jets.[22]

Since the literature has shown some differences in the acoustic characteristics of rectangular jets compared with circular jets, it is worthwhile to look at the basic fluid dynamic characteristics as well. Similar to round jets, rectangular jets are characterized by different flow regions. In general these include the core region, the transition region, and the fully-mixed turbulent region.[28] The core is characterized by an unmixed region just downstream of the nozzle exit. Eventually, this disappears due to the merging of the shear layers. In a round jet, this is well defined since the shear layer is axisymmetric. However, in the case of a rectangular jet the issue is somewhat clouded. If one assumes the two dimensions to be independent, there are shear layers that grow on each of the 4 edges. The two shear layers associated with the small dimension will merge at a different location downstream than the two from the large dimension. The core is typically defined as the location where the centerline velocity falls below a certain value, usually 99% of the exit velocity. Therefore, a definite length can be associated with the core. However, one must keep in mind that the shear layers are much more complex than the round jet case.

The transition region in a rectangular jet is a region of high mixing where the jet flow is still essentially considered a 2-dimensional flow. As the flow continues downstream, the mixing eventually causes the flow to become axisymmetric. This indicates the beginning of the fully mixed region. In this region, the flow has many characteristics similar to a circular jet, including the centerline velocity decay rate proportional to x^{-1} (streamwise distance).[28] The length of the core region is dependent on the jet Mach number and temperature.[28] The velocity centerline decay has also been shown to be a function of the aspect-ratio.[28]

The region where the highest level of noise is produced in a jet is in the mixing layer around the core region.[28] This is where the shear is very high, and the associated velocities are also at their highest. Well downstream the flow evolves into a round jet flow, however the flow velocities are much lower than the exit condition and therefore do not radiate jet noise at comparable levels to the near exit region.[28] However, as with round jets there are many theories that have been proposed. In addition to studying round jets, Tam has investigated other nozzle shapes including rectangular jets. In his studies he has limited his research to low aspect-ratio nozzles. His results indicate that rectangular jets are actually similar to round jets.[7,9-12] References [7,9-12] show Tam's fits do indeed agree well with the experimental data. This indicates that round jet noise and rectangular jet noise are actually very similar since both can be fit to one set of generic spectral curves.

As is evident by the variation in data and theories, there is still much to be investigated in the area of rectangular jet noise. The aspect- ratios considered 'high' in the above discussion are typically one or two orders of magnitude lower than the typical aspect-ratio of the HARN system of the present study. Thus, there is definitely a need to generate some clean, systematic very high aspect-ratio noise data so that theories can be extended to this realm.

Results

Adaptation of Lighthill's Acoustic Analogy for Rectangular Jets

Lighthill's analogy for aerodynamic comes from the solution of the linearized flow equations. The acoustic pressure is found to be

$$p \sim \iiint_V \frac{\partial^2}{\partial t^2} T_{ij}\, \partial V . \tag{6}$$

By assuming

$$\frac{\partial^2}{\partial t^2} \sim \omega^2 \sim \left(\frac{U}{L}\right)^2 \tag{7}$$

$$T_{ij} \sim \rho u_i u_j \sim \rho U^2 \tag{8}$$

$$\partial V \sim AL \tag{9}$$

It can be shown that the acoustic intensity is

$$I \sim p^2 \sim \left[\rho U^4 \frac{AL}{L^2}\right]^2 \tag{10}$$

where U is the freestream velocity and L is a characteristic length-scale of the flow in the axial direction. Typically, the differential volume is assumed to be proportional to the cross-sectional area of the nozzle and the axial length-scale, $dV \sim AL$. For a round jet, $L \sim D$ and $A \sim D^2$. In the case of the HARN, $A \sim hw$ and Larsen[30], in his adaptation of Lighthill's jet noise prediction scheme, stated that the axial and cross-direction length-scales were both proportional to nozzle height, $L \sim h$. Thus, substituting these values into the differential volume definition, $dV \sim h^2 w$. The resulting proportionality for the intensity of the jet noise becomes

$$I \sim p^2 \sim \left[\rho U^4 \frac{h^2 w}{h^2}\right]^2 \sim \rho^2 U^8 \frac{h^4 w^2}{h^4} \sim \rho^2 U^8 w^2 . \tag{11}$$

Interestingly, the sound intensity appears to be proportional to the square of the width and not proportional to the nozzle height at all. This is not what has been found in the HARN data or by others.

Thus, the adaptation of Lighthill's scaling equation to rectangular jet noise is not as simple as it initially appeared.

Rather than attempting to completely re-evaluate the terms in the acoustic pressure equation to achieve an adapted intensity relationship, we will assume that the eddy volume and length scale will produce a relationship similar to that for the round jet noise case, in that $I \sim L^2$. Using the OASPL data L_{eq} can be defined as it was in reference [1]. This seems as though it is an ad-hoc way of resolving the problem, however its validity can be checked by using the defined length scale in the Strouhal number and examining how well the spectra collapse. Figure 1(b) shows typical HARN acoustic spectra scaled according to the defined equivalent length. It is noted that the relationship collapses the data reasonably well, although there it can be seen that the scaling has not completely removed the effect of nozzle width.

To further examine the differences between the noise data at different widths, the OASPL is plotted verses the aspect-ratio of the nozzle in figure 2. The data for all three widths appear to have similar trends, with slopes varying from 1.6 to 2.1. However, perhaps a more direct comparison is to remove the change in SPL due to the nozzle area. Round jet noise has been found to scale with nozzle area. Similarly, figure 3 shows the same HARN data from figure 2 with an additional factor subtracted out to account for the change in noise due to change in area. This produces an interesting result.

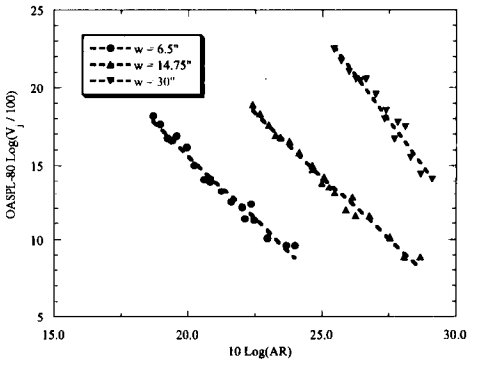

Figure 2: HARN OASPL data versus aspect-ratio, AR = (w / h).

Rather than having three independent curves based on different widths, the two smaller widths appear to fall along the same trend-line in the plot. The largest width, w = 30", however does not collapse in the same manner. Two possible scenarios exist: (1) there is a significant change in the jet flow between w = 15" and w = 30", or (2) there is a consistent error in the w = 30" data. All aspects of the experiments were examined to verify the quality of the data. No error, or inconsistency was found in the experiment, or the data. One possible problem that may have affected the data was the relatively short distance between the nozzle exit and the jet collector in the chamber. Due to the size of the HARN, the distance from the HARN exit and the collector inlet was only 7 ft. Thus, the location of the collector was only at x/w = 2.8 for w = 30". In the width dimension, the collector is only 4' wide. Thus, it was possible that the jet may have impacted the sides of the collector inlet. How much noise might be produced in this case is unknown, however the collector is covered in acoustic foam. For the other two nozzle widths the x/w was about 6 and 13, respectively. This could be a possible cause of the different trend for the w = 30" case.

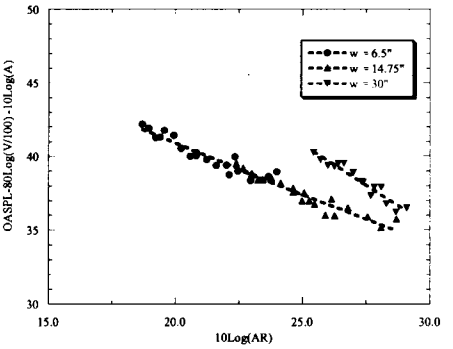

Figure 3: HARN OASPL corrected for jet velocity and nozzle area versus aspect-ratio.

An attempt at obtaining the best fit for the effect of aspect ratio showed that the OASPL was proportional to $AR^{-1/2}$. The data is shown in figure 4 corrected using all the parameters discussed thus far. This collapses the OASPL data at $\Theta = 90^{\circ}$ to within +/- 2 dB. For the two smaller widths, the scheme improves, collapsing the data to within +/- 1 dB.

APPENDIX E

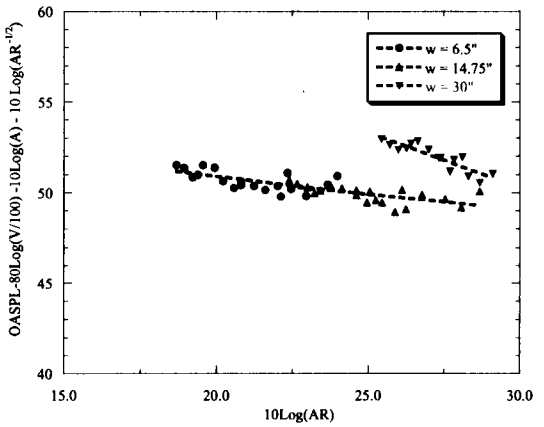

Figure 4: Best fit scaling to OASPL data based on aspect-ratio.

Improvements to Prediction of Jet-Noise at Low Polar Angles

It has been well documented that at low polar angles the high frequency sound undergoes refraction, scattering, and absorption by mixing layer turbulence.[5] This is because the high frequency noise is generated very close to the nozzle exit and then must pass through a large portion of the turbulent jet in order to arrive at the microphone. If the turbulence scale is on the order of the wavelength of the noise there can be significant amounts of absorption and scattering.[5] Thus, when compared to prediction schemes that do not account for this effect, the data does not coincide with what is expected from the prediction.

Referring to the prediction scheme based upon Lighthill's theory for round jets, the sound intensity is given by

$$I \sim \frac{\rho_m^2 V_j^8 D^2}{\rho_o a_o^5 R^2}(1 - M_c \cos(\Theta))^{-5}. \quad (12)$$

Notice that the only term that varies with polar angle is the convection amplification term, $(1 - M_c \cos \Theta)^{-5}$. This involves the convection Mach number of the turbulent eddies. Typically most researchers assume $M_c \sim 0.65\ M_j$. However, it was shown by the present authors in reference [2], that the convection velocity decreased with increased distance from the nozzle. It was found that the convection velocity was generally in the range of $0.65V_j$. It was also shown in reference [2] that $V_\ell/V_j \sim (x/h)^{-1/2}$ beyond the core.

This information can be used to calculate a more accurate convection Mach number for the entire noise-producing region of a jet. Given that

$$M_c = \frac{V_c}{a}, \quad (13)$$

and multiplying by $\frac{V_\ell}{V_\ell}\frac{V_j}{V_j}$, the convection Mach number can be re-arranged into the form

$$M_c = \frac{V_c}{a}\frac{V_\ell}{V_\ell}\frac{V_j}{V_j} = \frac{V_c}{V_\ell}\frac{V_\ell}{V_j}\frac{V_j}{a} \sim 0.65\frac{V_\ell}{V_j}M_j, \quad (14)$$

since $V_c/V_\ell \sim 0.65$. The maximum is 0.65 due to the fact that $V_\ell/V_j < 1$ beyond the core region of the jet. Since the noise producing region of a jet is on the order of 20 x/h and the core length is on the order of 4 x/h, a constant value of $M_c = 0.65\ M_j$ is not a representative value for the entire noise producing region. Unfortunately, the form of the convection Mach number shown in equation (14) is not implemented easily into most prediction schemes that assume a constant convection Mach number for agiven jet exoit Mach number. However, an average M_c, over the entire noise producing region, can easily be calculated and used in prediction schemes that only allow a constant M_c. In the case of the HARN, it was shown $V_\ell/V_j \sim (x/h)^{-1/2}$. Taking the average of V_ℓ/V_j from x/h = 0 to x/h = 20 results in $[V_\ell/V_j]_{ave} \sim 0.55$. Thus, an improved constant value convection Mach number (for a fixed M_j for the HARN, based on equation (14) is $M_c = (0.65)(0.55)M_j = 0.36M_j$.

Figure 5 shows some comparisons between using the original and new values of M_c. There is an obvious improvement in the data, however it has still not collapsed into one curve that could be used for prediction. One might think that this type of correction would only improve the low frequency portion of the spectrum, since much of the low frequency noise is produced downstream of the tip of the potential core. On the other hand, the high frequency noise is presumed to be produced near the nozzle exit and upstream of the tip of the potential core Thus, the convection velocity for high frequencies should be on the order of $0.65M_j$. However, there is a vast improvement in the collapse of the data from using the lower convection Mach number.

APPENDIX E

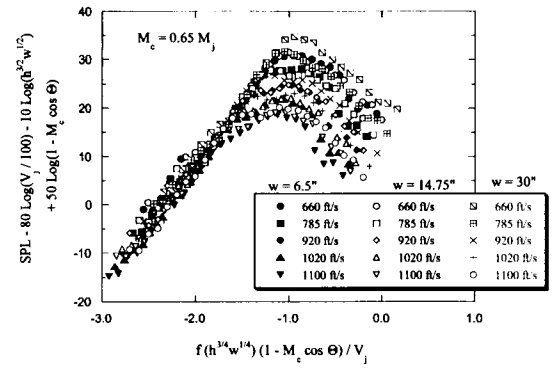

(a)

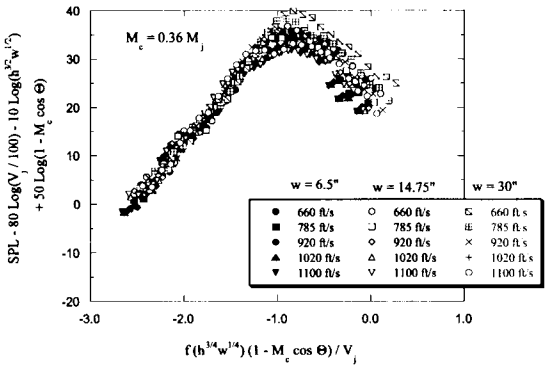

(b)

Figure 5: HARN acoustic data at $\Theta = 20^\circ$, (a) $M_c = 0.65\ M_j$, (b) $M_c = 0.36\ M_j$.

Possible explanation for these observations can be explained using the source location data by others of both the round and rectangular nozzles. The source locations of the HARN were examined using available data in the literature to better estimate the value for convection Mach number. In their effort to develop a new source location methodology, Ahuja, Massey, and D'Agostino performed a study for round nozzles[31] to determine the streamwise source locations of different frequencies as a function of fD/V_j. Like a number of earlier studies on jet noise source location, they found that high frequency noise tended to be generated near the nozzle, while lower frequency noise was generated further downstream.[31] It should also be noted that similar trends were found in recent (unpublished at the time of writing of this paper) source location results on low aspect-ratio rectangular nozzles obtained at GTRI using fh/V_j as the Strouhal number.

For comparison, the maximum and minimum values for Strouhal number for all the HARN data were calculated to determine a general range of Strouhal number for the HARN tests. Strouhal numbers for the HARN ranged from $fh/V_j = 0.0002$ to 1.02 ($f_{min}\ h_{min} / V_{max}$ to $f_{max}\ h_{max}/V_{min}$). From the data in reference [31] and recent low aspect-ratio rectangular nozzle source location data, it was determined that even the frequencies with the highest Strouhal numbers were associated with sources at at least 5 nozzle heights downstream from the nozzle exit, and therefore beyond the core region of the jet.

Larsen[30] also reported results for his nozzle at Strouhal numbers, fh/V_j of 0.5 and 0.1. He showed that most of the noise was generated at downstream distances > 5h, and in the case of the lower Strouhal number the noise producing region was significant as far away from the nozzle as $x/h \sim 25$. This tends to indicate that the majority of the high frequency HARN noise is produced downstream of the core. Thus, even the high frequency noise that was measured needs the convection velocity adjustment described earlier. Hence, this could be a reason why the M_c adjustment improves the data at the higher frequencies. Thus it is assumed that $M_c = 0.36M_j$. It is a reasonable average convection Mach number when all frequency sources are considered, and explains the improved collapse seen in figure 5. It should be pointed out that it is likely, that in our case, the noise produced very near the nozzle exit is at frequencies beyond the measurement capability of the microphone system used. The data acquisition system used in the experiments was only able to acquire data up to 100 kHz. This in combination with the lowest velocity tested of 660 ft/s and the largest slot height of 0.080" only produces a Strouhal number of 1.02 for a frequency of 100 kHz. Thus, the highest frequency sources recorded are located around $x/h > 5$. This tends to indicate that all the noise generated from sources located at $x/h < 5$ will have higher frequencies and are therefore are not recorded in the data. This is supported by examining the HARN data at $\Theta = 90^\circ$. Notice that the spectra are very flat, and never tend to roll-off at high frequency as one might expect based on other jet noise data. Therefore, it is probable that the recorded spectra and the actual spectra should actually extend well beyond the 100 kHz limit of the frequency analyzer as depicted in figure 6. Because of this fact, it should be noted that the OASPL data for the HARN maybe somewhat lower than it should be. Therefore data from a larger nozzle, where the entire frequency spectrum is recorded, will most likely have a higher OASPL value when compared to HARN data. In the example shown in figure 6, this difference is small, only by about 1 dB. There could be a more pronounced difference in the OASPL values if the peak value of the HARN spectrum at a particular

condition was at a frequency higher than the maximum recorded frequency.

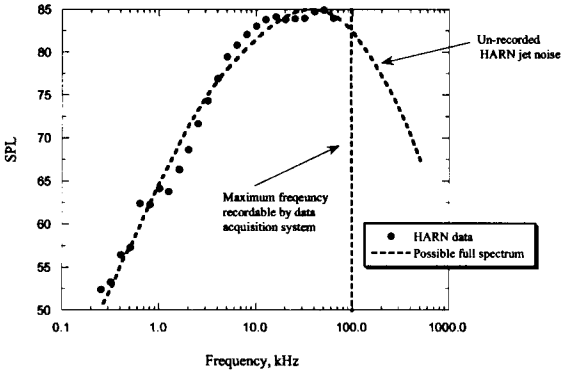

Figure 6: Depiction of possible HARN jet noise beyond the frequency range capabilities of the data acquisition system.

Based on the HARN acoustic and fluid dynamic data, a reasonable collapse of the OASPL and the frequency spectra has been obtained. For high aspect-ratio rectangular jet noise, it has been found that the sound intensity is given by

$$I \sim \frac{\rho_m^2 V_j^8 L_{eq}^2}{\rho_o a_o^5 R^2}(1 - M_c \cos(\Theta))^{-5} \quad (15)$$

where M_c is a function of frequency and x/h; and $L_{eq} = (h^{3/4} w^{1/4})$. The basic form of the equation is similar to the equation for sound intensity developed for round jets. Other researchers have used equivalent diameter as the characteristic length scale, however, the HARN data did not follow $I \sim D_{eq}^2$ where $D_{eq} = (4hw/\pi)^{1/2}$. Finally, it was found that some simple improvements to the estimation of the convection Mach number also improved the prediction of the noise at low polar angles.

Although this prediction scheme collapsed the high aspect-ratio data quite well, it is still desirable to develop a prediction scheme that can relate round jet noise and rectangular jet noise. This would enable the wealth of data for round jet noise to be used for jet noise prediction for rectangular jets. Thus, in the following section, HARN jet noise will be compared with round jet noise data and an attempt will be made to develop one set of scaling parameters that predict noise levels for either geometry.

Comparison of HARN Jet Noise with Round Jet Noise.

Since most of the available experimental data and literature concerning jet noise is associated with round nozzles, it is desirable to compare and scale the HARN results with those for round nozzles. If a relationship between the two types of jet-noise could be established, all the theory and correlations used for round jet noise could be applied to rectangular jet noise using this relationship as a bridge.

Ahuja and Bushell[4] and Lush[16] were some of the first experimenters that made an attempt to verify the relationships developed by Lighthill. Ahuja and Bushell tested 3 different diameter round nozzles at several different jet velocities and made acoustic measurements at several different polar angles.[4] Ahuja found mixed results when trying to compare his data with Lighthill's theory.[5] At high polar angles he was able to collapse data for different velocities and nozzle diameters using Lighthill's relationships. However, at small polar angles, the data did not collapse at high frequency. Figures 7 and 8 are representative figures from reference [4] and are typical results. Figure 7 shows that the jet noise does indeed scale for polar angles above 60°. However, figure 8 shows that there is relatively poor collapse at the lower polar angles, particularly at higher frequencies. Ahuja suggested that this was due to absorption and scattering of the high frequency noise by the turbulent eddies of the shear layer, through which sound arriving at a microphone at a low polar angle would have to travel.[5] Using his data, Ahuja developed two prediction schemes, one for low frequencies below the peak frequency and a different prediction scheme for frequencies higher than the peak value.

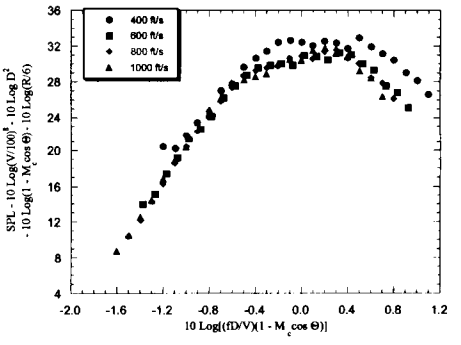

Figure 7: Ahuja round jet data from reference [4], D = 2.84", high polar angles.

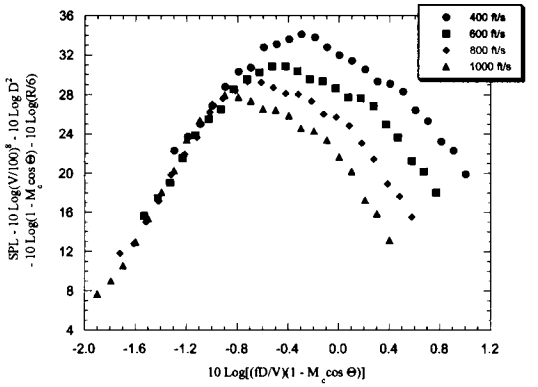

Figure 8: Ahuja round jet data from reference [4], D = 2.40", $\Theta = 30^{\circ}$.

Similar scaling parameters have been found for the HARN and collapsing the data showed similar results. In the previous sections the noise prediction scheme was improved by using observations from the HARN data and by using results from fluid dynamic measurements. Some easy to implement improvements were made that drastically improved the prediction and the scaling of the HARN data. Lighthill's scaling for the HARN with the length-scale replaced by L_{eq} is

$$I \sim \frac{\rho_m^2 V_j^8 L_{eq}^2}{\rho_o a_o^5 R^2}(1 - M_c \cos(\Theta))^{-5}, \qquad (16)$$

where the convection Mach number is a function of the frequency and the location of the source of the sound in the flow. Equation (11) can be re-arranged into a more convenient form using the area and the aspect ratio rather than L_{eq},

$$I \sim \frac{\rho_m^2 V_j^8 A(AR)^{-1/2}}{\rho_o a_o^5 R^2}(1 - M_c \cos(\Theta))^{-5},$$

where AR = w/h. (17)

Since the adapted equation is a better prediction of the noise for the HARN jet, it stands to reason that this new equation may improve round jet noise results as well. The round jet data used for the comparison will be the data of Ahuja and Bushell from reference [4]. It is easiest to use equation (17) since substituting $A \sim D^2$ and AR = 1 for a round jet reduces equation (17) to the well-known sound intensity relationship for round jets.

The same source location data was used to determine the locations associated with the different frequencies for the round jet data. Figure 9 is the data from figure 8 with the modified M_c. As it turns out, the addition of the improved convection Mach number does not improve the scaling of the round jet data. Since it has shown to produce a significant improvement in the case of the HARN, it requires further examination.

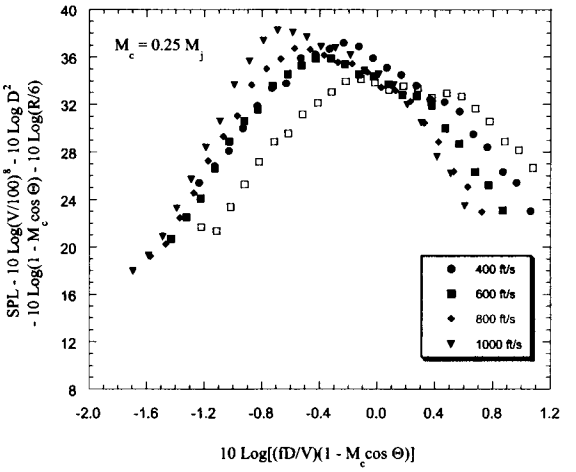

Figure 9: Round jet noise data scaled using modified convection Mach number.

Figure 10 shows sample calculated source locations for the jet noise for the round nozzle data and the HARN based on the data from reference [31]. Notice that the HARN range of Strouhal numbers indicates that the noise sources are well downstream of the nozzle exit while the round jet has a significant number of the sources in its frequency range located in the region of the jet core. In the fluid dynamic study of the HARN, it was found that the convection velocity decreased as distance from the nozzle increased. Thus, since sources of different frequencies are located at different streamwise locations, different frequencies will have different convection velocities. Figure 11 shows the convection velocity of the noise sources based on their location. Notice that the sources for the round jet noise data span a wide range of streamwise locations from the nozzle exit to several diameters downstream of the core. This would possibly explain the different results between the HARN and the round jet.

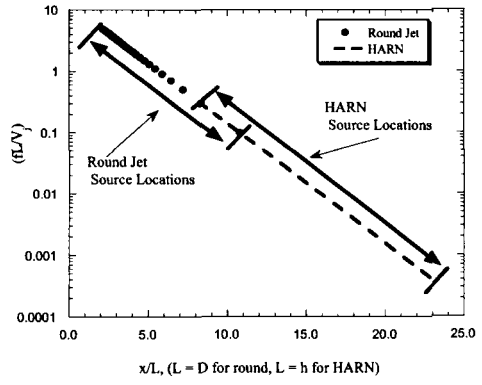

Figure 10: Source locations for HARN and round jet noise based on data from reference [31].

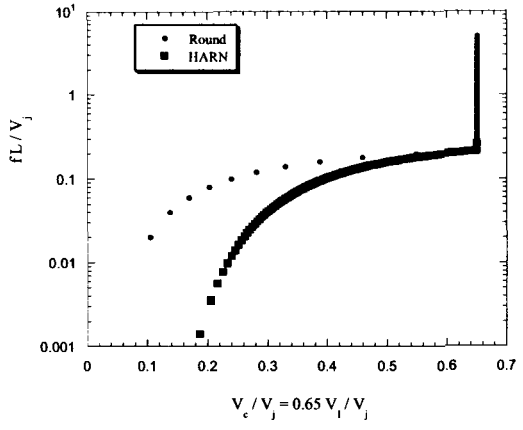

Figure 11: Convection velocities of turbulent eddies based on source location.

Since the round jet data has sources in the region near the nozzle exit, modifying the convection Mach number may not improve the data collapse. However, in the case of the HARN, where much of the noise generated near the nozzle exit appears to be at frequencies beyond the capability of the data acquisition system, the sources associated with the recorded data are located mostly downstream of the core. Therefore, there was a major benefit to modifying the convection Mach number to a value more appropriate for the sources.

Figure 12 shows both the HARN and round nozzle jet noise data scaled according equation (17). The frequency has been normalized by the respective length scale for each set of data, i.e., L = D for the round data, and L = L_{eq} for the HARN data. Thus, one scaling equation has been used to collapse both sets of data. Notice that the data sets are similar, however, they do not have similar peak frequencies and levels. It is apparent that the two configurations do not completely collapse into one curve using the parameters discussed. This figure also supports the argument that a significant portion of the HARN data is not recorded by the data acquisition system since the HARN spectra appear to be similar to half of a round jet noise spectra.

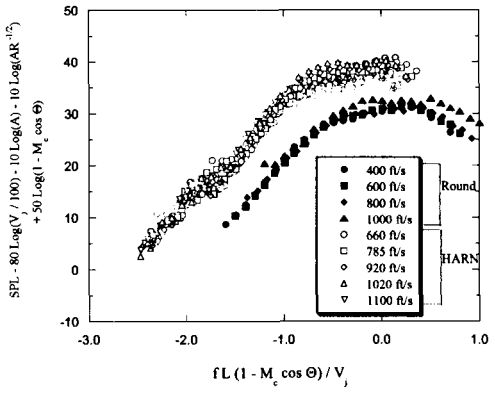

Figure 12: HARN and round nozzle data scaled using the same parameters.

The HARN and the round nozzle curves have similar shapes, but appear to be shifted. This indicates that the two types of jet noise may be related, but that the particular scaling parameters used here are not completely appropriate for collapsing the two data sets. More work will have to be done in this area to improve this result. In particular, systematic data examining the aspect-ratio contribution to jet noise may help clarify the relationship.

In summary, scaling from Lighthill's equation was adapted to estimate the noise levels of the HARN acoustic data. Some modifications were also made to the convection Mach number term based upon the findings from the fluid dynamic portion[2] of the present study. This new prediction scheme was then applied to HARN and classic round jet noise data. The new prediction scheme was found to improve the collapse of only the HARN data at lower polar angles, but the modified convection Mach number did not improve the collapse of the round jet noise data. The two sets of data were then directly compared using a common scaling equation. It was found that the common scaling equation did not quite collapse both sets of data to one curve. Since the spectral shapes are similar, it does appear possible to collapse the two types of jet noise data with an improved scaling relationship.

APPENDIX E

Comparison of HARN Data to Tam's Generic Jet Noise Spectra.

Although Lighthill's theory has been around for many years, there is still a great amount of controversy as to whether or not the theory based on acoustic analogy is in fact valid. The V_j^8 law and the relationship between the noise and the diameter of a round jet have been well documented in experiments. However, the Doppler shift term remains questionable since data scaled by this term does not seem to collapse with varying polar angle.

Recently, Tam et al. have suggested some reasoning behind the discrepancy.[6-13] They suggested that the reason high polar angles and low polar angles do not collapse is because they are associated with different types of noise.[6-13] Tam et al. broke down the jet noise into two components: one associated with the large-scale structures and from the other associated with the fine-scale turbulence.[10-13] He contends that the large-scale structures radiate predominately in the downstream direction, i.e., low polar angles, while the fine-scale turbulence noise dominates at the higher polar angles.[10-13] Tam et al argue that since there are two mechanisms generating the noise at the different angles, there is no reason why they should scale in the same manner, and hence there should be two distinct spectra associated with the different mechanisms.

This argument was backed up by Tam by generating curve fits to several sets of experimental data under many different conditions.[10-13] These empirical fits are generic jet noise spectra that are particular to the direction of radiation. One curve represents jet noise radiated at low polar angles and is associated with the large-scale turbulence of the jet flow, while the other is valid for higher polar angles, and hence is the result of fine-scale turbulence noise.]

Tam has expanded his theory beyond round jets.[9, 11, 12, 13] Tam contends that the shape of the jet noise spectra will not change even for varying geometry.[9] He has with some success been able to show that his generic spectra fit experimental data for nozzle geometries other than round. He does however qualify this extension only to "reasonable" geometries that include geometries that would not create a significant thrust loss compared with a round nozzle.[11]

Since Tam has had success in comparing his generic jet noise spectra to many types of jet noise data, it is useful to compare Tam's generic jet noise spectra with the HARN data. This can help support Tam's case that the jet noise spectrum shape is independent of nozzle configuration.[11] It would also expand this theory to an extreme geometric case where he has not yet attempted to apply his generic spectra.

The generic spectra functions are generated as a function of f/f_p (f_p = peak frequency) and can be found in several of Tam's references.[9-13] The functions were programmed into a Matlab script file and are presented in figure 13. Notice that the peak is at a non-dimensional frequency of $f/f_p = 1$ and that the peak amplitude is normalized to zero. It should also be noted that Tam generated these curves from narrowband data reduced to the power spectral density (PSD, Δf = 1 Hz). This fit cannot be generated by simply using f/f_p based on 1/3-octave bands and be expected to be appropriate. In fact in references [6-13], for comparison to experimental data the generic curves were left in narrowband frequencies and 1/3-octave jet noise data was converted back to narrowband for comparison.

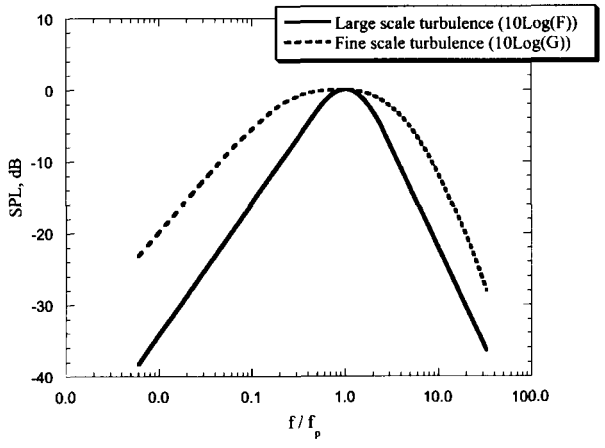

Figure 13: Tam's generic jet noise spectra (reproduced from equations in reference[9]).

In the case of the HARN, narrowband data was available, however significant effort had already been taken to compare all data in 1/3-octave bands so it could be readily compared with older classic experiments. Suddenly switching to comparing data in narrowband would change the peak amplitude, frequency, and shape of the spectra that have already been presented and discussed. Thus it was decided to transform Tam's generic curve fits to 1/3-octave spectra.

Figure 14 shows Tam's curves converted to 1/3-octave bands with the frequencies f_p = 1000 Hz. The equations can be re-scaled and at this point these generic curves can be compared with experimental data in 1/3-octave bands. Initially Tam's curves will be compared with HARN data by simply shifting HARN data by subtracting off the peak amplitude and dividing the frequency by the peak frequency. Once this general comparison has been performed, an attempt will be made to use an empirical prediction fit to predict the peak frequency and amplitude of HARN spectra.

APPENDIX E

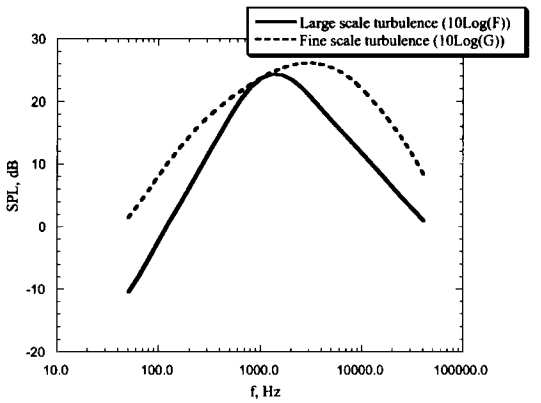

Figure 14: Tam's generic jet noise spectra converted to 1/3 octave bands from the PSD with f_p = 1000 Hz.

For the HARN data, the large-scale generic spectrum will be compared with experimental data at polar angles at $\Theta = 30^\circ$ while the fine-scale turbulence generic spectrum will be compared with HARN data for $\Theta = 90^\circ$. Figure 15 shows a comparison between Tam's curves and HARN data. Several HARN spectra are shown in the figure normalized by their peak SPL and frequency. Thus, several HARN curves can be directly compared to the generic spectra on one plot.

The large-scale curve is used to compare with the 30° data, while the fine-scale curve is used to compare with 90° data. A combination of both curves is used to examine 60° data. In general, it appears that the curves do tend to represent the shape of the spectra at high and low polar angles, and the mid-range angles appear to be a combination of both curves. These results are in agreement with Tam's conclusions.

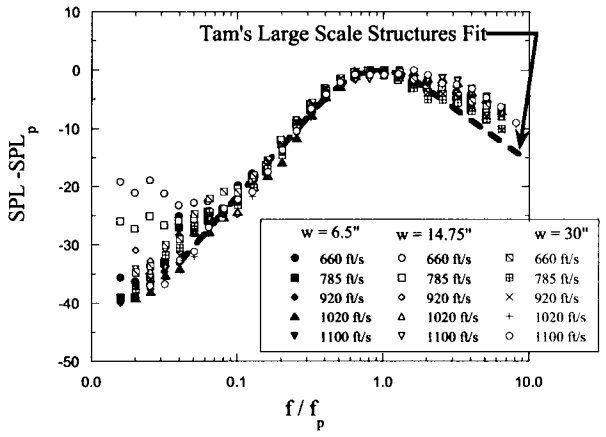

(a)

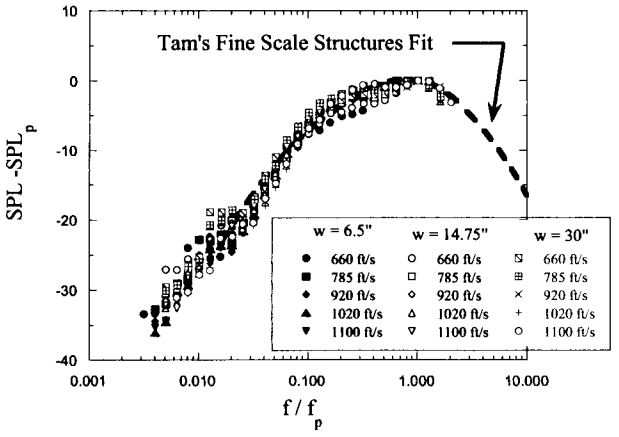

(b)

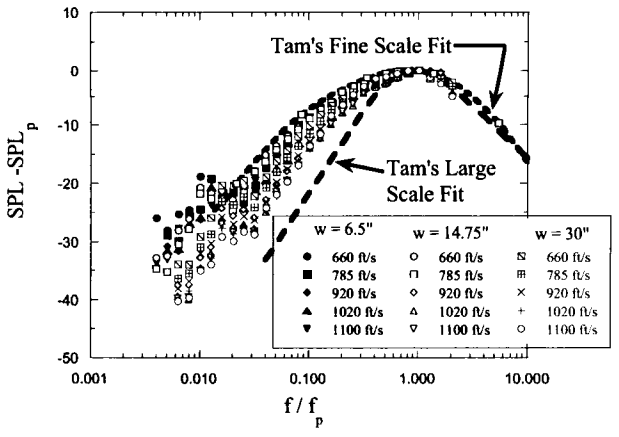

(c)

Figure 15: Typical HARN data compared to Tam's corresponding curves, (a) $\Theta = 30^\circ$, (a) $\Theta = 90^\circ$, (c) $\Theta = 60^\circ$.

APPENDIX E

Summary

From the HARN acoustic and fluid dynamic data there were some basic trends that had been identified. The acoustic data was found to vary with V_j^8. An equivalent length was also defined to parallel round jet scaling based on Lighthill's equation, which contains a length dimension squared. No direct relationship was immediately apparent between L_{eq} and h and w. A "best-fit" to the data was used to define L_{eq} making the sound intensity proportional to L_{eq}^2. The relationship found was $L_{eq} = h^{3/4}w^{1/4}$.

Since this was a rather unlikely scaling-parameter, a more in-depth examination of the OASPL data's variation with h and w was carried out. The prediction scheme was re-arranged into a form containing area and aspect ratio rather than L_{eq} ($I \sim (A(AR)^{-1/2}$, note $A(AR)^{-1/2} = L_{eq}^2$). This provided a direct way of scaling both round jet noise and HARN jet noise using the same scaling equation.

In addition to the scaling parameter associated with the geometry, the fluid dynamic data revealed that the convection Mach number was not necessarily 0.65 M_j. In fact, M_c varied with distance downstream of the nozzle and actually was found to be proportional to the local centerline velocity of the jet, V_t. Thus, over much of the noise-producing region of the jet, the average M_c is much lower than $0.65M_j$.

In addition, it was found that M_c/M_t was also a function of frequency. Other researchers have shown that different frequencies are generated at different downstream locations in the jet flow. These facts were used to generate an improved convection Mach number estimation. These changes to the estimates from Lighthill's equation improved the collapse of HARN acoustic data, particularly at low polar angles where the convection Mach number has the greatest effect.

This data was also compared with classic round jet acoustic data using the same modifications in order to make the comparison using a common prediction scheme. The two very different nozzles produced similar results in many ways. Both jets follow the V_j^8 law and have a similar spectral shape and were found to have similar amplitudes when scaled by the developed prediction scheme. The amount of agreement was surprising since the geometries were so vastly different. However, the modified convection Mach number did not improve the collapse of the round jet data used in the comparison. This is believed to be due to the fact that the high frequency noise from the round jet is produced near the jet exit, thus a significant portion of the spectra actually is associated with a convection Mach number of 0.65 M_j. However, in the case of the HARN, collapse was improved because it is believed that the noise generated close to the exit of the HARN had such high frequencies that it was beyond the capabilities of the data acquisition system. Thus, the majority of the noise recorded in the spectra is associated with turbulence with much lower convection Mach numbers downstream of the core region of the jet.

The HARN acoustic data was also compared with Tam's generic jet noise spectra. Tam's generic curves predicted the shape of the spectra quite well. In general, the HARN data was found to collapse using a modified version of the round jet scaling parameters derived from Lighthill's equation.

References

1. Munro, Scott E. and Ahuja, K. K., "Aeroacoustics of a High Aspect- Ratio Jet," AIAA-2003-3323, 2003, presented at the 9th AIAA/CEAS Aeroacoustics Conference and Exhibit, Hilton Head, South Carolina, USA, 12 - 14 May 2003.
2. Munro, Scott E. and Ahuja, K. K., "Fluid Dynamics of a High Aspect- Ratio Jet," AIAA-2003-3129, 2003, presented at the 9th AIAA/CEAS Aeroacoustics Conference and Exhibit, Hilton Head, South Carolina, USA, 12 - 14 May 2003.
3. Munro, Scott Edward, "Jet Noise of High Aspect-Ratio Rectangular Nozzles with Application to Pneumatic High-Lift Devices." Georgia Institute of Technology, PhD thesis, January, 2002.
4. Ahuja, K.K., and Bushell, K.W., "An Experimental Study of Subsonic Jet Noise and Comparison with Theory." Journal of Sound and Vibration, Vol. 30, No. 3, pp. 317-341, 1973.
5. Ahuja , K.K., "Correlation and Prediction of Jet Noise." Journal of Sound and Vibration, Vol 29, No. 2, pp. 155-168, 1973.
6. Tam, C.K.W., Golebiowski, M., and Seiner, J. M., "On the Two Components of turbulent Mixing Noise from Supersonic Jets." AIAA Aeroacoustics Conference, AIAA paper 96-1716, May 1996.
7. Tam, Christopher K.W., "Influence of Nozzle Geometry on the Noise of High-Speed Jets." AIAA Journal, Vol. 36, No. 8, pp. 1396 – 1400, August 1998.
8. Tam, Christopher K.W., and Laurent, Auriault, "Jet Mixing Noise from Fine Scale Turbulence." AIAA paper 98-2354.
9. Tam, Christopher K.W., "Influence of Nozzle Geometry on the Noise of High-Speed Jets." AIAA paper 98-2255, 1998.
10. Tam, C.K.W., and Zaman, K.B.M.Q., "Subsonic Jet Noise from Non-Axisymmetric and Tabbed Nozzles." AIAA Aerospace Sciences Meeting, AIAA paper 99-0077, January 1999.

APPENDIX E

11. Tam, Christopher K.W., and Zaman, K.B.M.Q., "Subsonic Jet Noise from Nonaxisymmetric and Tabbed Nozzles." AIAA Journal, Vol. 38, No. 4, pp. 592 – 599, April 2000.
12. Tam, Christopher K.W., and Pastoouchenko, Nikolai, "Noise from the Fine Scale Turbulence of Nonaxisymmetric Jets." AIAA Aeroacoustics Conference, AIAA paper 2001-2187, May 2001.
13. Tam, Christopher K.W., "On the Failure of the Acoustic analogy Theory to Identify the Correct Noise Sources." AIAA Aeroacoustics Conference, AIAA paper 2001-2117, May 2001.
14. Lighthill, M.J. "On sound Generated Aerodynamically. I. General Theory," Proceedings of the Royal Society A 211, pp 564-578, 1952.
15. Lighthill, M.J. "On sound Generated Aerodynamically. II. Turbulence as a Source of Sound," Proceedings of the Royal Society A 222, pp 1-21, 1954.
16. Lighthill, M.J. "Jet Noise," North Atlantic Treaty Organization Advisory Group for Aeronautical Research and Development, Report 448, 1963.
17. Lighthill, M.J. "Jet Noise," AIAA Journal, Vol. 1 Number 7, pp. 1507-1517, 1963.
18. Tyler, J. M., Sofrin, T. G., Davis, J. W., "Rectangular Nozzles for Jet Noise Suppression," SAE National Aeronautic Meeting, April 1959.
19. Capone, F. J., and Maiden, D. L., "Performance of Twin Two-Dimensional Wedge Nozzles Including Trhust Vectoring and Reversin Effects at Speeds up to Mach 2.20," NASA TN D-8449, 1977.
20. Capone, F. J., Hunt, B. L., and Path, G. E., "Subsonic/Supersonic Nonvectored Aeropropulsive Characteristics of Nonaxisymmetric Nozzles Installed on an F-18 Model." AIAA Paper 81-1445. 1981.
21. Seiner, John M., Ponton, Michael K., Manning, James C., "Acoustic Properties Associated with Rectangular Geometry Supersonic Nozzles," AIAA Paper 86-1472, 1986.
22. Kouts, C. A., and Yu, J. C., "Far Noise Field of a Two-Dimensional Subsonic Jet." AIAA Journal Vol. 3, No. 8, pp. 1031 – 1035. August 1975.
23. Maglieri, D. J., and Hubbard, H. H., "Preliminary Measurements of the Noise Characteristics of Some Jet Augmented Flap Configurations." NASA Memo 12-4-58L, 1958.
24. Coles, W. D., "Jet Engine Exhaust from Slot Nozzles." NASA TN D-60, 1959.
25. Maestrello, L., and McDaid, E., "Acoustic Characteristics of a High-Subsonic Jet." AIAA Journal, Vol. 9, No. 6, pp. 1058-1066, 1971.
26. Gruschka, H. D., and Schrecker, G. O., "Aeroacoustic Characteristics of Jet Flap Type Exhausts." AIAA Paper 72-130, 1972.
27. Schrecker, G. O., and Maus, J. R., "Noise Characteristics of Jet Flap Type Exhaust Flows." NASA Grant, NGR 43-001-075, 1975.
28. Olsen, W. A., Butierrez, O., and Dorsch, R. G., "The Effect of Nozzle Inlet Shape, Lip Thickness, and Exit Shape and Size on Subsonic Jet Noise." AIAA Paper 73-187, 1973.
29. Ffowcs-Williams, J. E., "Some Open Questions on the Jet Noise Problem." Boeing Science research Lab. Doc., DL-82-0730, 1968.
30. Larsen, P. N., "Noise Generated by Air Jets from a Rectangular Slit." Ph.D. Thesis, Technical University of Denmark, 1983.
31. Ahuja, K. K., Massey, K. C., D'Agostino, M. S., "A Simple Technique of Locating Noise Sources of a Jet Under Simulated Forward Motion." 4th AIAA/CEAS Aeroacoustics Conference, AIAA 98-2359, 1998.
32. Lush, P. A., "Measurement of Subsonic Jet Noise and Comparison with Theory." Journal of Fluid Mechanics, Vol. 46, pp. 477-500, 1971.